Article

Neuron

Spinal Locomotor Circuits Develop Using Hierarchical Rules Based on Motorneuron Position and Identity

Highlights

- Large-scale imaging reveals spinally driven motor column-specific activity patterns
- Motorneuron subtype identity and position are dispensable for rhythmic activity
- Perturbation of motorneuron subtype identity alters muscle coordination circuitry
- Distinct modules of spinal motor circuitry are wired hierarchically

Authors

Christopher A. Hinckley, William A. Alaynick, Benjamin W. Gallarda, ..., Haley O. Tucker, Tatyana O. Sharpee, Samuel L. Pfaff

Correspondence

pfaff@salk.edu

In Brief

Hinckley et al. use GCaMP6 imaging and mouse genetics to perturb motorneuron development in order to disentangle different regulatory layers of the spinal motor circuitry. They find that motorneuron subtype identity is required to ensure that proper control of intralimb muscle coordination is established.

Hinckley et al., 2015, Neuron *87*, 1008–1021
September 2, 2015
http://dx.doi.org/10.1016/j.neuron.2015.08.005

CellPress

CellPress

Neuron
Article

Spinal Locomotor Circuits Develop Using Hierarchical Rules Based on Motorneuron Position and Identity

Christopher A. Hinckley,[1] William A. Alaynick,[1] Benjamin W. Gallarda,[1] Marito Hayashi,[1] Kathryn L. Hilde,[1] Shawn P. Driscoll,[1] Joseph D. Dekker,[2] Haley O. Tucker,[2] Tatyana O. Sharpee,[1,3] and Samuel L. Pfaff[1,*]

[1]Gene Expression Laboratory and the Howard Hughes Medical Institute, Salk Institute for Biological Studies, 10010 North Torrey Pines, La Jolla, CA 92037, USA

[2]Institute of Cellular and Molecular Biology, The University of Texas at Austin, Austin, TX 78712, USA

[3]Computational Neurobiology Laboratory, Salk Institute for Biological Studies, 10010 North Torrey Pines, La Jolla, CA 92037, USA

*Correspondence: pfaff@salk.edu

http://dx.doi.org/10.1016/j.neuron.2015.08.005

SUMMARY

The coordination of multi-muscle movements originates in the circuitry that regulates the firing patterns of spinal motorneurons. Sensory neurons rely on the musculotopic organization of motorneurons to establish orderly connections, prompting us to examine whether the intraspinal circuitry that coordinates motor activity likewise uses cell position as an internal wiring reference. We generated a motorneuron-specific GCaMP6f mouse line and employed two-photon imaging to monitor the activity of lumbar motorneurons. We show that the central pattern generator neural network coordinately drives rhythmic columnar-specific motorneuron bursts at distinct phases of the locomotor cycle. Using multiple genetic strategies to perturb the subtype identity and orderly position of motorneurons, we found that neurons retained their rhythmic activity—but cell position was decoupled from the normal phasing pattern underlying flexion and extension. These findings suggest a hierarchical basis of motor circuit formation that relies on increasingly stringent matching of neuronal identity and position.

INTRODUCTION

Movement relies on neuronal circuits that coordinate the activity of motorneuron subtypes controlling different muscles. This is achieved by precisely controlling the relative timing of muscle flexion and extension at multiple limb joints, while simultaneously counteracting the forces on the body axis to maintain balance and posture. Motorneuron subtypes become organized into a musculotopic pattern during development, meaning that the relative position of each motorneuron soma corresponds to the relative position of their muscle target in the periphery (Romanes, 1941, 1951; Landmesser and Morris, 1975). This stereotyped organization of motorneurons has long been thought to be a possible substrate for facilitating the connectivity of pre-motor inputs that control and coordinate movement (Jessell et al., 2011). The formation of the musculotopic motor map is intrinsically programmed by an intricate genetic system that specifies the subtype identity of motorneurons and controls soma migration, axon targeting, dendritic pattern, and sensory connectivity (Dasen and Jessell 2009; Ladle et al., 2007; Bonanomi and Pfaff, 2010). How these complementary positional and genetic factors influence the wiring of inputs to control the fine pattern and coordination of motorneuron firing to achieve complex motor behaviors remains poorly understood.

Motorneurons in the lumbar spinal cord can be broadly divided into two anatomically and genetically defined subclasses. Those controlling axial musculature are positioned within the medial motor column (MMC), whereas the motorneurons controlling limb muscles are situated in the lateral motor column (LMC). The LMC is further divided into lateral (LMCl) and medial (LMCm) subdivisions that innervate muscles within the dorsal and ventral limb buds, respectively (Hollyday, 1980). Initially lumbar motorneurons transition through a ground state in which Isl1 and Lhx3 are coexpressed to create primitive MMC-like cells that are the precursors for each motor column (Sharma et al., 1998). Part of the columnar diversification process is driven by Foxp1, which triggers LMC development leading to the downregulation of Lhx3 and activation of Lhx1 expression in the LMCl and Isl1/2 in the LMCm (Rousso et al., 2008; Dasen et al., 2008). The LMCl and LMCm columns are comprised of multiple motor pools that control muscles for flexion and extension of limb joints during locomotion. Thus, the inter- and intra-column coordination of motorneuron activity is a critical regulatory feature that ensures proper motor control.

Motorneurons receive inputs from a variety of sources ranging from sensory afferents that detect tension in muscles and tendons, to descending motor commands from higher brain centers for initiating volitional movements. However, the rhythmic activation of hind limb muscles used during stepping is driven by a network of lumbar spinal interneurons called the locomotor central pattern generator (CPG; Kiehn 2006; McCrea and Rybak, 2008), so named because the CPG is an autonomous spinal patterning circuit that drives rhythmic motor bursts alternating between right and left limbs, while coordinating flexion and

extension movements to produce swing and stance of the limb during each step cycle. The CPG consists of several classes of interneurons including V0, V1, V2a, V2b, V3, and dI6 populations that each have specific molecular, cellular, and physiological signatures and form a complex circuit with direct and indirect inputs to motorneurons (Stepien and Arber, 2008; Grillner and Jessell, 2009; Garcia-Campmany et al., 2010; Goulding, 2009). Functional studies in mice have revealed a remarkable degree of modularity in the CPG circuit, finding that V0 cells regulate left-right alternation, V1 neurons control the frequency of the step cycle, and V2a and V3 cells control the precision and robustness of the motor output (Talpalar et al., 2013; Lanuza et al., 2004; Gosgnach et al., 2006; Crone et al., 2009; Zhang et al., 2008). Interestingly, retrograde viral tracing suggests that MMC and LMC cells receive different presynaptic inputs (Goetz et al., 2015). The cellular and molecular features that govern locomotor CPG neuron connectivity to motorneuron subtypes within each column are not known but logically might follow some of the principles identified for sensory afferent inputs. In some cases stringent genetic cues such as Sema3e help to directly control afferent connectivity (Pecho-Vrieseling et al., 2009; Fukuhara et al., 2013); however, there are also systems that indirectly influence sensory-motor connectivity based on using cell position coordinates to select synaptic partners (Sürmeli et al., 2011). Thus, it is difficult to predict a priori whether pre-motor input from the spinal circuitry involved in coordinating motorneuron activity is established using instructive genetic cues or passive recognition mechanisms, and in particular whether all components of the CPG use the same wiring strategy.

It has been challenging to identify what features of motorneuron subtype identity contribute to CPG connectivity because electrophysiological recording methods have primarily focused on monitoring the composite activity of many cells by recording from the ventral root comprised of mixed motorneuron subtypes. Conversely, single-cell recordings to examine motor coordination are challenging because it is difficult to determine the activity-relationship between many motorneurons simultaneously. In this study, we have overcome these limitations using the genetically encoded calcium indicator GCaMP6f and two-photon imaging to simultaneously monitor the activity of LMC and MMC motorneuron subtypes. We found that, regardless of subtype identity, the vast majority of motorneurons become rhythmically active and alternate in a left-right stepping-like pattern when the CPG is chemically activated. As expected, the motor activity evoked by the CPG produced stereotypical phases of bursting within the MMC, LMCl, and LMCm, corresponding to the patterned regulation that underlies hind limb flexion-extension and postural control. Next, we exploited the known genetics that control motorneuron diversification to alter LMC-neuron position and identity by either deleting *Foxp1* to prevent LMC formation (*Foxp1*$^{\Delta MN}$) or sustaining Lhx3 to promote MMC development (*Lhx3*^{ON}). Surprisingly, *Lhx3*^{ON} motorneurons retained their rhythmic bursts and left-right coordination regardless of their position in the ventral horn, suggesting neither position nor subtype identity are critical determinants for establishing this layer of CPG control over motorneurons. In contrast, the inter-columnar phasic pattern of motorneuron activity was disrupted in *Lhx3*^{ON} mice. Taken together, these findings reveal a modular strategy for establishing CPG control over the motor system. Functionally distinct circuit elements for rhythmic drive, left-right coordination, and swing-stance limb and axial coordination are independently assembled according to a hierarchy of rules for each circuit element involving distinct contributions from generic motorneuron identity, columnar cell position, and motorneuron subtype identity.

RESULTS

GCaMP6f Accurately Reveals Spinal Motorneuron Activity

In order to examine the mechanisms that coordinately regulate the activity of motorneurons, we sought to develop an optical method that would allow us to accurately monitor large numbers of these neurons. We generated a transgenic mouse line expressing GCaMP6f under the control of the Hb9 motorneuron-specific promoter (*Hb9::GCaMP6f*) and tested the sensitivity and fidelity of this reporter for neuronal activity (Thaler et al., 1999; Lee et al., 2004; Chen et al., 2013). As expected GCaMP6f fluorescence was detected in a majority (~85%) of the ChAT+ motorneurons in transgenic *Hb9::GCaMP6f* embryonic day 18.5–postnatal day 2 (E18.5–P2) spinal cords. The relative intensity of ChAT and GCaMP6f varied slightly among cells likely because the *Hb9* promoter is more active in some motorneuron subtypes (Figures S1A, S1B, and S2; William et al., 2003). *Hb9::GCaMP6f* transgenic mice appeared normal, suggesting that the GCaMP6f reporter did not significantly alter motor function. GCaMP6f baseline fluorescence was detected within the intact spinal cord of live tissue under unstimulated conditions and individual motorneurons within both the lateral and medial portions of the LMC and MMC could be well resolved using either confocal or two-photon microscopy (Figure S2; see below). Thus, the *Hb9::GCaMP6f* reporter is well suited for labeling the majority of lumbar motorneurons and does not appear to markedly alter motor function.

To determine whether GCaMP6f fluorescence intensity was an accurate and sensitive surrogate for measuring neuronal activity, we antidromically evoked motorneuron spikes by electrically stimulating the ventral roots while recording GCaMP6f optical signals with two-photon microscopy. In late embryonic and early postnatal spinal cords (E18.5–P2), a train of four electrical stimuli to a single ventral root generated optical responses in >90% of the imaged segmental motorneurons (Figure 1A). Furthermore, a substantial majority of motorneurons robustly responded to single stimuli (Figure 1A; 64.3% ± 9%, 257 motorneurons, n = 3 spinal cords), suggesting the fluorescence signals generated by GCaMP6f in response to calcium were sufficient to reliably detect small numbers of action potentials in motorneurons within both the MMC and LMC, though the signal amplitude appeared to be lower in MMC cells (Figure 1A). Increasing numbers of ventral root stimuli at 10 Hz evoked linearly increasing response amplitudes across a range from 1 to 16 stimuli, further suggesting GCaMP6f is a wide dynamic range reporter for motorneuron activity (Figure 1B). To examine the temporal summation of GCaMP6f signals, we characterized the responses of motorneurons by varying the frequency of antidromic stimulation. Images were acquired at 8.3 frames/s with a field of view

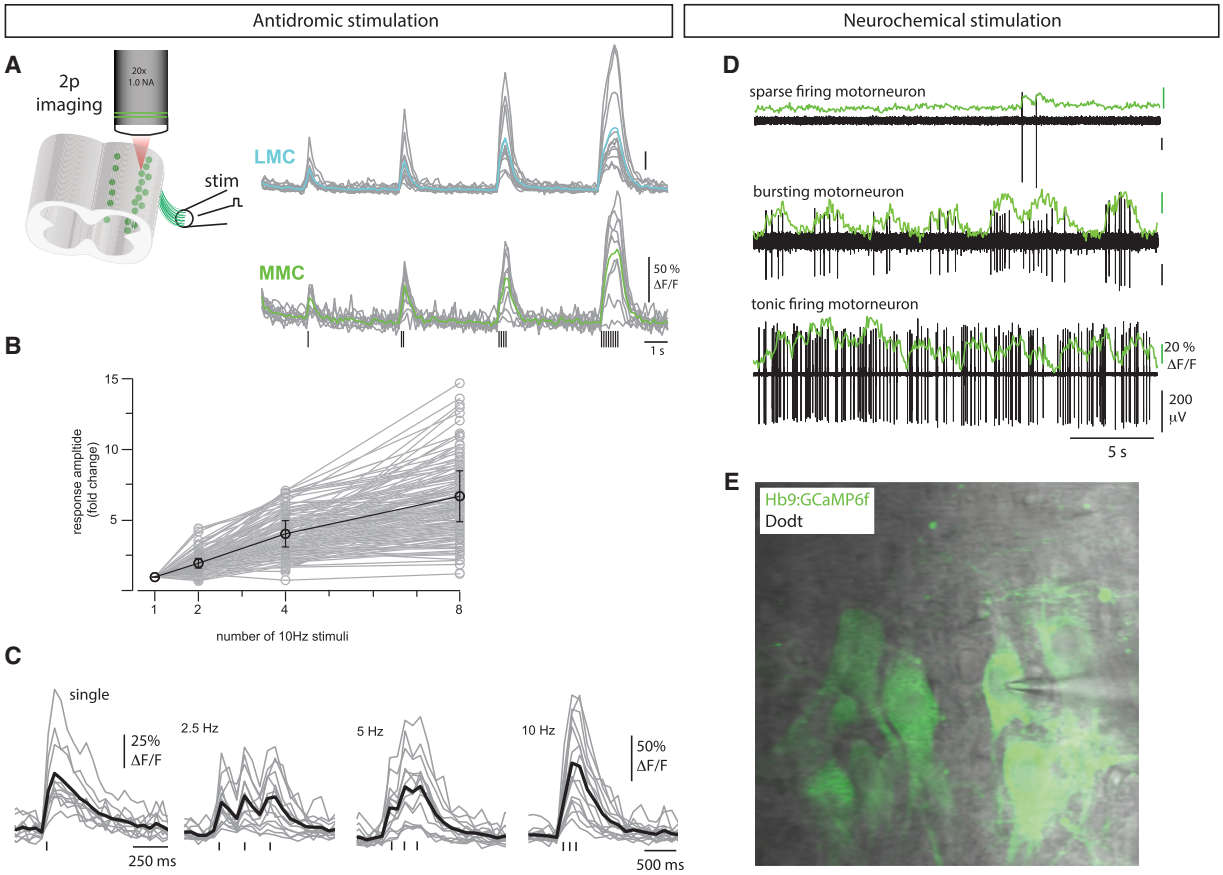

Figure 1. GCaMP6f Reliably Reports Neural Activity in Spinal Motorneurons

(A) Electrical stimulation of the ventral root (black ticks) evoked calcium signals in LMC (cyan) and MMC (green) motorneurons. Increasing numbers of stimuli evoked larger-amplitude, longer-duration responses. LMC and MMC motorneurons respond with similar kinetics and summation to ventral root stimulation, but signals are larger in the LMC. Inset, diagram of experimental setup. Hb9:GCaMP6f signals were imaged through the ventral surface of the spinal cord.

(B) Increasing numbers of stimuli evoked a linear increase in the response amplitude of spinal motorneurons. Amplitudes normalized to response amplitude of the single stimulus ΔF/F. Means ± SD.

(C) Single stimuli evoked fast rising, exponentially decaying responses. Trains of 3 stimuli at 2.5 and 5 Hz evoked separable fluorescence peaks corresponding to each stimulus with temporal summation. Stimulation at rates faster than the imaging frame rate (10 Hz stimuli, 8.3 Hz imaging) generated larger responses without detectable peaks from individual stimuli.

(D) Examples of neurochemically (NMA and serotonin) evoked motorneuron electrical and GCaMP6f signals in individual motorneurons. Electrical signals (black) and raw imaging signals (green) are superimposed. Motorneuron activity-related GCaMP6f fluorescence signals are evident for isolated single spikes (top), spike bursts (middle), and tonic firing (bottom).

(E) Phase contrast (Dodt) and fluorescence image of visually targeted cell-attached recording from a GCaMP6f-expressing motorneuron (bursting cell in top panel).

of ~550 × 550 μm to visualize signals across the MMC and LMC columns of intact spinal cords. We observed temporal summation of GCaMP6f responses with superimposed individual spike responses at 2.5 Hz and 5 Hz, which fused into a single response following 10 Hz stimulation (Figure 1C). These results indicate that the GCaMP6f responses we detect are a temporal summation of the calcium signals associated with bursts of action potentials in motorneurons.

Although these experiments indicate that GCaMP6f reliably reports evoked spike trains, the responses to network-evoked activity were not known. To correlate the activity of individual motorneurons with imaging signals, we performed cell-attached recordings from GCaMP6f-expressing motorneurons (Figures 1D and 1E, n = 6). Neurochemical (NMA and serotonin)-evoked excitation of the spinal cord triggered a variety of electrically recorded firing patterns in lumbar motorneurons ranging from sparse activity to bursting and tonic firing (Figure 1D). In the absence of motorneuron spiking, imaging signals were devoid of large-amplitude, fast rising, exponentially decaying signals (Figure 1D, upper trace). Imaging signals during motorneuron bursting or fluctuations in tonic firing were well correlated with the timing and relative firing rates of the recorded motorneurons (Figure 1D, middle and bottom traces). By narrowing the field of view and increasing the acquisition speed to 14.8 frames/s individual spike transients could be resolved (Figure 1D, upper and middle traces). This characterization suggests that GCaMP6f

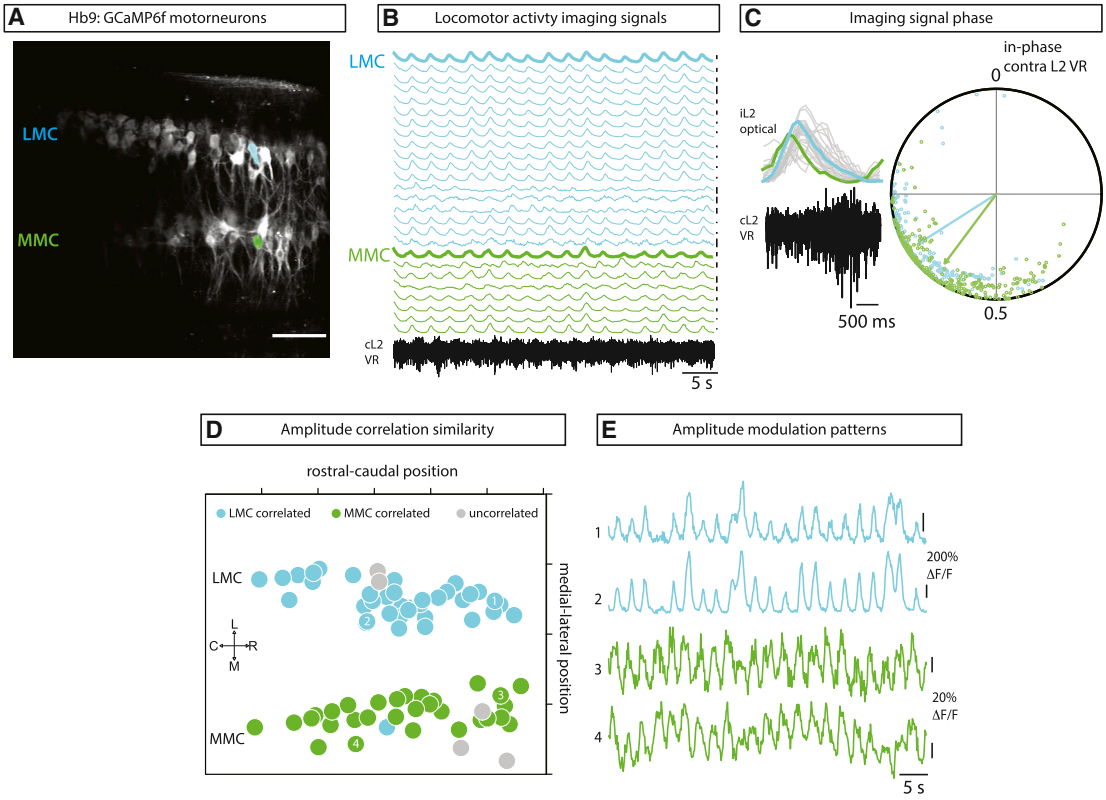

Figure 2. Comparison of LMC and MMC Locomotor Oscillations

(A) Single optical section of Hb9:GCaMP6f expressing motorneurons in L2. Example LMC and MMC neurons are highlighted in cyan and green, respectively. Lateral is up and rostral is right. Scale bar, 100 μm.

(B) Raw imaging signals from the motorneurons in (A). Following neurochemical induction of fictive locomotor activity (10 μM NMA and 20 μM 5HT) fluorescence oscillations in LMC (cyan traces) and MMC (green traces) alternate with the electrically recorded activity in the contralateral L2 ventral root (bottom, black trace). Traces from LMC and MMC neurons highlighted in (A) are bold. Scale bar, 100% ΔF/F.

(C) Left: expanded single locomotor cycle with overlaid imaging traces and contralateral ventral root electrical activity. L2 Imaging oscillations alternate with the contralateral L2 ventral root bursting. Right: polar plot of imaging signal phase calculated relative to bursting in the contralateral L2 ventral root. Points are individual L2 motorneurons.

(D) Schematic of motorneuron positions and amplitude correlations in a single L2 optical section. Points represent motorneuron soma positions colored according to relative strength of their correlations to LMC (cyan) or MMC (green). A majority of motorneurons are more strongly correlated within a motor column than across motor columns.

(E) Example traces from pairs of LMC and MMC neurons numbered in D. Amplitude modulation patterns for motorneurons within the same column were more similar than those across motorneuron columns.

imaging of spinal motorneurons reliably reports spiking activity across a range of firing rates and imaging speeds.

Motorneurons within the LMC and MMC Display Different Patterns of Activity

Classic studies of the CPG have recorded the population responses of motorneuron activity from the ventral root, where the axons of MMC and LMC motor neurons both exit the spinal cord together (Smith and Feldman, 1987; Kjaerulff and Kiehn, 1996). In contrast, the CPG-driven activity of individual motorneurons within each motor column has remained unknown until recently (Machado et al., 2015). We first established that NMA and serotonin reliably activate the CPG network in spinal cords from E18.5–P2 *Hb9::GCaMP6f* transgenic mice. These preparations displayed rhythmic, well-coordinated fictive locomotion represented by alternating left-right and L2-L5 ventral root activity (data not shown). Following activation of the CPG two-photon imaging of GCaMP6f revealed that the majority of motorneurons displayed clear fluorescence oscillations (84% ± 10.5%; 5,144 motorneurons, n = 7 spinal cords) that corresponded to the same frequency of oscillations detected by recording from the contralateral ventral roots (Figures 2A and 2B). Thus, this optical method allowed measurement of the motor activity driven by the CPG with single-cell resolution across multiple motorneuron subtypes. In addition, this revealed that most motorneurons respond to CPG driven activity, rather than a special subset.

Imaging the L2 ventral spinal cord revealed both the MMC and the LMC motor columns (Figure S1). This allowed us to compare the frequency and phase of motorneuron-bursting within these two columns simultaneously under conditions of drug-evoked CPG activation. MMC and LMC motorneurons at L2 displayed similar bursting frequencies and alternated with the contralateral

L2 ventral root (Figures 2B and 2C). Interestingly, at this spinal level both MMC and LMC motorneurons burst in the same phase (Figure 2C). By convention L2 motorneuron activity in wild-type mice is defined as flexor-motor activity (Kiehn and Kjaerulff, 1996). Although cells within the LMC and MMC had similar properties with regard to rhythmicity, bursting frequency, and phase, we reasoned that there might be subtle differences in the activity of LMC and MMC cells because cellular tracing studies have found their spinal inputs are different (Goetz et al., 2015). We used a graph-based analysis to examine the correlations in cycle-to-cycle amplitude variation between all motorneuron pairs (see Experimental Procedures). This analysis revealed that the majority of motorneurons within either the LMC or the MMC displayed a strong co-variant amplitude pattern, whereas motorneurons in different columns did not co-vary in burst amplitude (Figures 2D and 2E). Together, these findings indicate that MMC and LMC motorneurons within the L2 spinal cord share many aspects of CPG co-regulation resulting in similar overall phasing of their bursts. Nevertheless, the distinct burst amplitude modulation patterns detected within the MMC and LMC also suggest that motorneurons within a column share similar activity profiles.

A primary trait of locomotor activity is the segregation of flexor and extensor activity along the rostrocaudal axis of the spinal cord (Yakovenko et al., 2002; Kiehn and Kjaerulff 1996). This anatomical feature of motorneurons predicts that cells with different relative phases of bursting will be found at specific rostrocaudal positions within the lumbar cord and that a phase transition in bursting should occur around L3-L4. To capture the activity of motorneurons across the lumbar spinal cord, we sequentially imaged GCaMP6f oscillations from multiple fields of view in L2, L3, L4, and L5 containing LMC motorneurons that control the hip, knee, and ankle muscles and MMC motorneurons of the lumbar epaxial muscles (Figure 3A; Figure S1). We registered the signals from different fields of view relative to a common ventral root electrical recording. As expected, we found that the activity pattern of the entire LMC at L2-L3 was in a different phase than the motor bursts of the LMC at L4-L5 (Figures 3A and 3B, cyan and orange traces). In contrast, MMC motorneurons retained the same phase from L2 to L5 (Figure 3B, green traces). These observations are consistent with EMG recordings of limb and axial muscles during quadrepedal walking (Schilling and Carrier, 2010). Importantly, these data provide evidence that the MMC and LMC display different phasic patterns of activity in the lower (L4-L5) lumbar spinal cord (Figures 3A and 3B).

Burst Phase Correlates with Cell Position

Next, we examined the activity of individual motorneurons to define the relationship between cell position and neuronal activity during fictive locomotion. Similar fractions of the LMC and MMC were rhythmically active (86.5% ± 10.7% of LMC; 77% ± 14.5% of MMC; $p = 0.47$) throughout the lumbar cord, suggesting that CPG-driven activity recruits motorneurons to a similar extent regardless of subtype identity or location. Among LMC neurons, we found that their activity coalesced into two dominant phase groups (Figures 3C and 3D, see Experimental Procedures). At upper lumbar levels (L2-L3) the majority of motorneurons were active during the flexor phase (87.9% ± 7.4%), whereas in lower lumbar levels (L4-L5) most LMC cells were extensor active (77.5% ± 21.7%). In contrast, MMC neurons were primarily active in the flexor phase regardless of lumbar level (Figures 3C and 3D).

To accurately assign motorneurons to the medial and lateral portions of the LMC, we performed intramuscular injections of fluorescent conjugated CTB into the gluteal muscle innervated by LMCl neurons and the hamstring innervated by LMCm motorneurons at P0 in *Hb9::GCaMP6f* animals. At mid-lumbar levels, L3-L4 the LMCm and LMCl are overlapped and the CTB labeling ensured an accurate assignment of the subdivision of the LMC (Figure S2). Imaging of GCaMP6f oscillations in L3 and L4 revealed that, following CPG activation, the medial-lateral subtype structure of the LMC was reflected in distinct activity patterns (Figures 4A–4C). We found that motorneurons within the LMCl were flexor active, while motorneurons in the LMCm were extensor active (Figure 4D; Movie S1).

These observations are consistent with the known muscle activation patterns recorded in vitro (Kiehn and Kjaerulff 1996; Hayes et al., 2009; Klein et al., 2010) and the stereotypical positions of hind limb motor pools in the mouse (McHanwell and Biscoe, 1981). To ensure that Hb9:GCamp6 expression levels, which vary between LMCm (low) and LMCl (high) did not bias our results (Figure S2), we performed a separate analysis of motorneuron activity recorded from *Isl1:Cre* x *ROSA:CAG:stop:GCaMP6f* animals in which GCaMP6f levels were evenly expressed within the medial/lateral subdivisions of the LMC (2072 motorneurons, n = 3 spinal cords). Similar to results with *Hb9::GCaMP6f* animals, we found that flexor-active motorneurons were located within the LMCl and extensor active cells in the LMCm (data not shown). We conclude that each motor column has a well-defined burst phase, which accordingly transforms the musculotopic position of motorneurons into an activity pattern for muscles.

CPG Activity with Altered Motorneuron Identity and Columnar Position

The correlation between burst phase and columnar position suggests that motorneuron cell position may be a major determinant in establishing the type of pre-synaptic input for motor control by the CPG. To test this hypothesis, we began by altering the relationship between motorneuron position and columnar identity. Foxp1 is a Hox-cofactor that is required for the proper specification of motorneuron subtypes (Dasen et al., 2008; Rousso et al., 2008). We crossed *Olig2:Cre* mice to *Foxp1*$^{fl/fl}$ animals to delete the *Foxp1* gene from motorneuron progenitors (*Foxp1*$^{\Delta MN}$). This genetic alteration allows motorneuron differentiation to progress but causes LMC cells to acquire hypaxial motorneuron (HMC) traits with a genetic signature typical of the thoracic neurons that innervate inter-rib musculature used during respiration. Thus, *Foxp1*- deletion leads to the generation of an ectopic thoracic subtype of motorneurons within the lumbar spinal cord, which we designate the HMC* (Dasen et al., 2008; Rousso et al., 2008). Within the P0 L3-L4 spinal cord of wild-type mice non-overlapping medial MMC and lateral LMC columns are apparent (Figures 5A, 5D, 5G, and 5J), whereas in *Foxp1*$^{\Delta MN}$ mutants HMC* neurons are shifted to an intermediate location normally devoid of motorneurons (Figure 5B, 5E, 5H, and 5K).

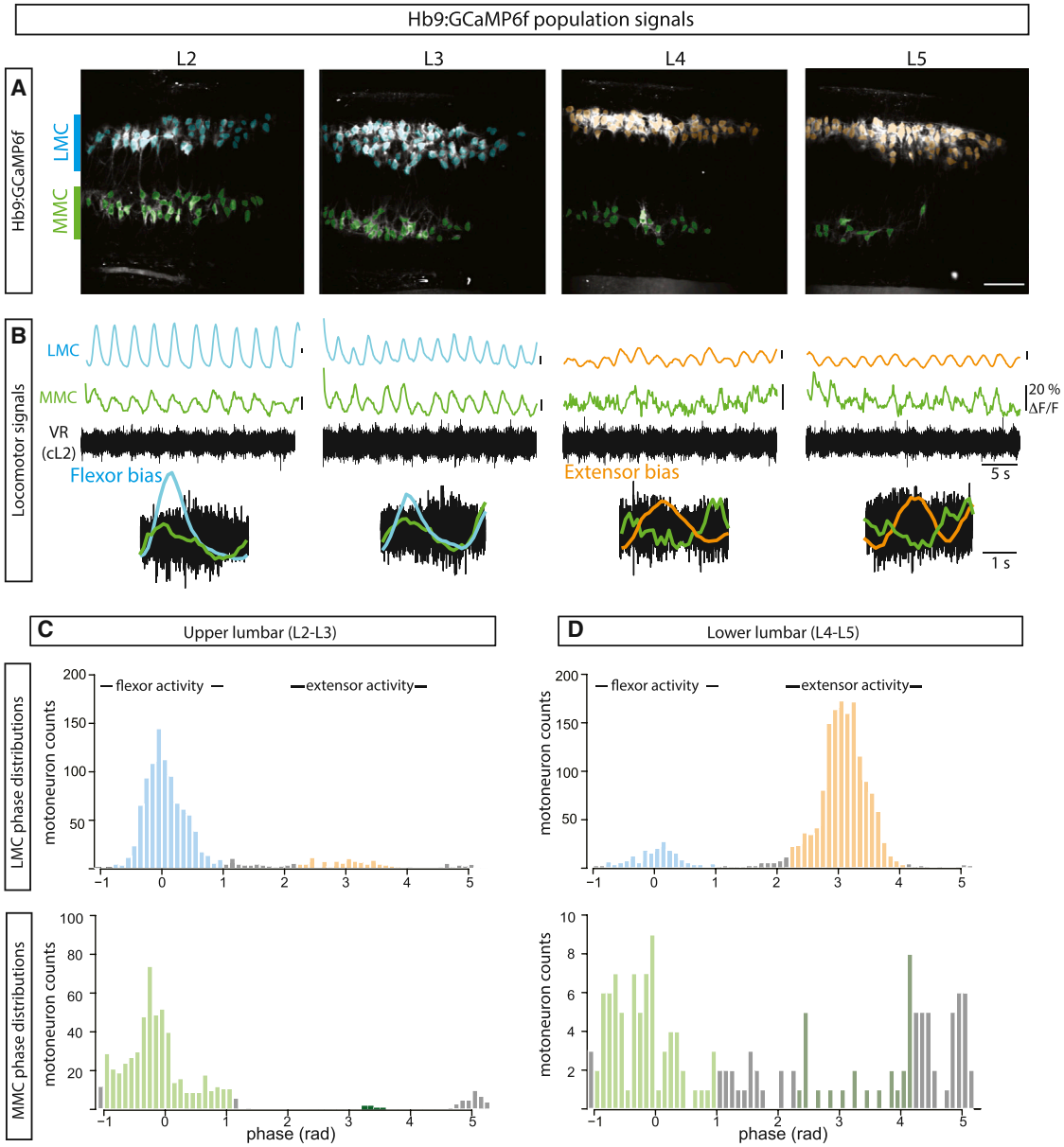

Figure 3. LMC and MMC Display Distinct Phase Patterns along the Rostral Caudal Axis

(A) Hb9:GCaMP6f images from lumbar segments L2–L5 highlighting LMC (L2-L3 cyan; L4-L5 orange) and MMC (green) motorneurons. Scale bar, 100 μm.

(B) Fluorescence intensity was measured across the population of neurons comprising each motor column. The phase of LMC motorneurons changes at the L3-L4 border (cyan to orange), while MMC neurons retain a similar phase along the lumbar enlargement. Below, LMC and MMC bursts superimposed over the contralateral L2 ventral root recording.

(C) Phase analysis of individual motorneuron imaging signals in the upper lumbar spinal cord. A majority of L2-L3 LMC motorneurons are flexor active with phase values centered around 0 radians (top). Similarly, a majority of MMC motorneurons are flexor active (bottom). A common color coding scheme is used for all remaining figures. Rhythmic neurons with phase values in the flexor range (0 ± 1 radians) are colored cyan for LMC and light green for MMC. Rhythmic neurons with phase values in the extensor range (π ± 1 radians) are colored orange for LMC and dark green for MMC. Rhythmic neurons with phase values outside the flexor and extensor ranges are colored gray.

(D) Phase analysis of individual motorneuron imaging signals in the lower lumbar spinal cord. A majority of L4-L5 LMC motorneurons are extensor active with phase values centered around π radians (77.5% ± 21.7%; orange, top). Fewer MMC neurons are present in L4-L5 lumbar levels than L2-L3, perhaps representing the transition from cells that control axial muscles to those involved in tail movements. A small but increasing fraction of extensor-active MMC cells are detected in L4-L5 (dark green) (14.7% ± 12%) relative to L2-L3.

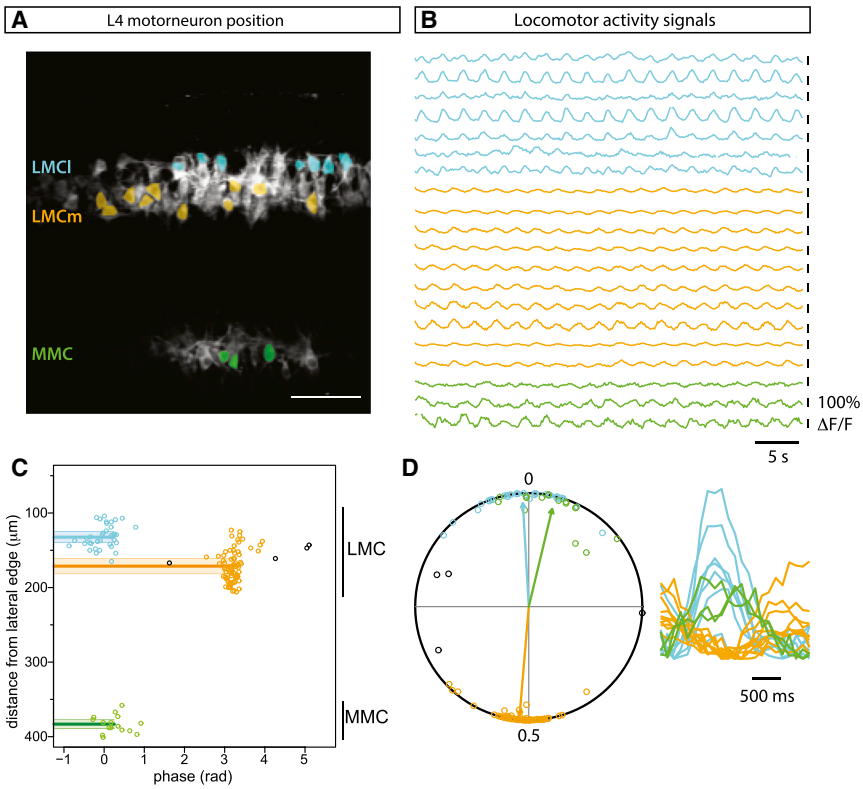

Figure 4. Intracolumnar Position Predicts LMC Motorneuron Activity

(A) Single optical section of Hb9:GCaMP6f expressing L4 motorneurons. Neurons in the LMCl and LMCm are highlighted in cyan and orange, respectively. MMC neurons are highlighted in green. Scale bar, 100 μm.

(B) Locomotor activity traces from motorneurons highlighted in (A). Two distinct phase groups are detected in the LMC. Flexor active the LMCl alternates with extensor active LMCm. MMC neurons (green) burst in phase with the LMCl (cyan).

(C) Scatterplot of motorneuron phase versus medio-lateral position separates three distinct motorneuron populations: LMCl, LMCm, and the MMC. Horizontal lines are mean ± SD of medio-lateral position for the phase categories.

(D) Polar plot of phase analysis from the motorneurons in (A). Two phase groups characterize L4 motorneuron activity, the LMCl and MMC (cyan, green) are in phase (flexor active), whereas the LMCm is shifted ~0.5 cycles (extensor active). Inset: overlaid signals from time series in (B) highlighting relative phases in a single locomotor cycle.

Neurochemical activation of the CPG in isolated spinal cords from E18.5–P0 *Foxp1*$^{\Delta MN}$ mutants reliably evoked rhythmic motor bursting recorded from the ventral roots, indicating that despite their ectopic position and altered subtype identity these motorneurons had received inputs from CPG circuitry (Figures 6A and 6B). The cycle period, cycle variation, and other parameters of ventral root bursting were remarkably similar between controls and *Foxp1*$^{\Delta MN}$ mutants (Figure 6C; cycle period p = 0.96; period variation p = 0.13; Figure S3), and normal left-right alternation was maintained (Figure 6D, p = 0.93). To rule out the possibility that the apparent normal pattern of motor activity detected in *Foxp1*$^{\Delta MN}$ animals was simply from Foxp1-independent MMC cells, we crossed *Foxp1*$^{\Delta MN}$ animals to *Hb9::GCaMP6f* transgenic mice and measured the fluorescence oscillations in individual MMC and HMC* motorneurons. We found that regardless of cell position motorneurons in *Foxp1*$^{\Delta MN}$ spinal cords were rhythmically active in similar fractions to wild-type motorneurons (Figures 6E and 6F; wild-type, 88.4% ± 10%; *Foxp1*$^{\Delta MN}$ 94% ± 3.3%, p = 0.09). These findings are consistent with recent studies using the GCaMP3 reporter (Machado et al., 2015) and indicate that motorneuron subtype identity and position are not critical determinants for establishing the CPG inputs that drive rhythmic left-right coordinated motor bursts.

Burst Phase Is Not Mandated by Cell Position

Although many aspects of CPG-driven motor activity appeared normal in *Foxp1*$^{\Delta MN}$ animals (Figure 6), ventral root recordings revealed that the coordination between L2 and L5 motorneurons was abnormal (Figure S3) (Machado et al., 2015). Across all lumbar levels, we found that the majority of HMC* were co-active with L2 cells, whereas the wild-type LMC was balanced with roughly equal contributions of neurons in and out of phase with L2 (HMC* 75.7% ± 8%; LMC 48.6% ± 11%). We sought to determine the burst-phase of the HMC* using the MMC as an internal reference since this motor column develops in a Foxp1-independent fashion (Figure 5K) (Rousso et al.,2008; Dasen et al., 2008). We found that the HMC* and MMC burst during the same phase throughout the lumbar cord, with similar fractions of the HMC* and MMC co-active with L2 (Figure 6G, p = 0.21). These data indicate that extensor-phase motorneurons are absent in *Foxp1*$^{\Delta MN}$ mutants (Machado et al., 2015) but raise the question whether this is due to the abnormal position or abnormal identity of HMC* motorneurons. Therefore, we sought a genetic strategy that would allow us to change the subtype identity of motorneurons while preserving their position in the LMC.

We manipulated the LIM-homeodomain transcription factor code to control motorneuron subtype diversification by preventing the downregulation of Lhx3 in motorneurons (Tsuchida et al., 1994; Sharma et al., 2000). *Hb9:stop:Lhx3* animals were crossed to *protamine:CRE* mice to generate embryos in which Lhx3 expression is maintained in motorneurons during embryogenesis (*Lhx3*^{ON}). Previous studies indicate that this manipulation keeps motorneurons in an MMC-like state based on their genetic profile and axon projection patterns (Sharma et al., 2000). Because *Lhx3*^{ON} mice die at birth from apparent motor and respiratory defects, we conducted our experiments with E18.5 embryos. When we examined the columnar location of motorneurons within *Lhx3*^{ON} mice, we found that the medial motor column was enlarged ~2- to 3-fold; however, many Hb9^{+} motorneurons were also located in lateral positions normally occupied by LMC neurons (Figure 5C, 5F, 5I, and 5L). Thus, *Lhx3*^{ON} mice contain

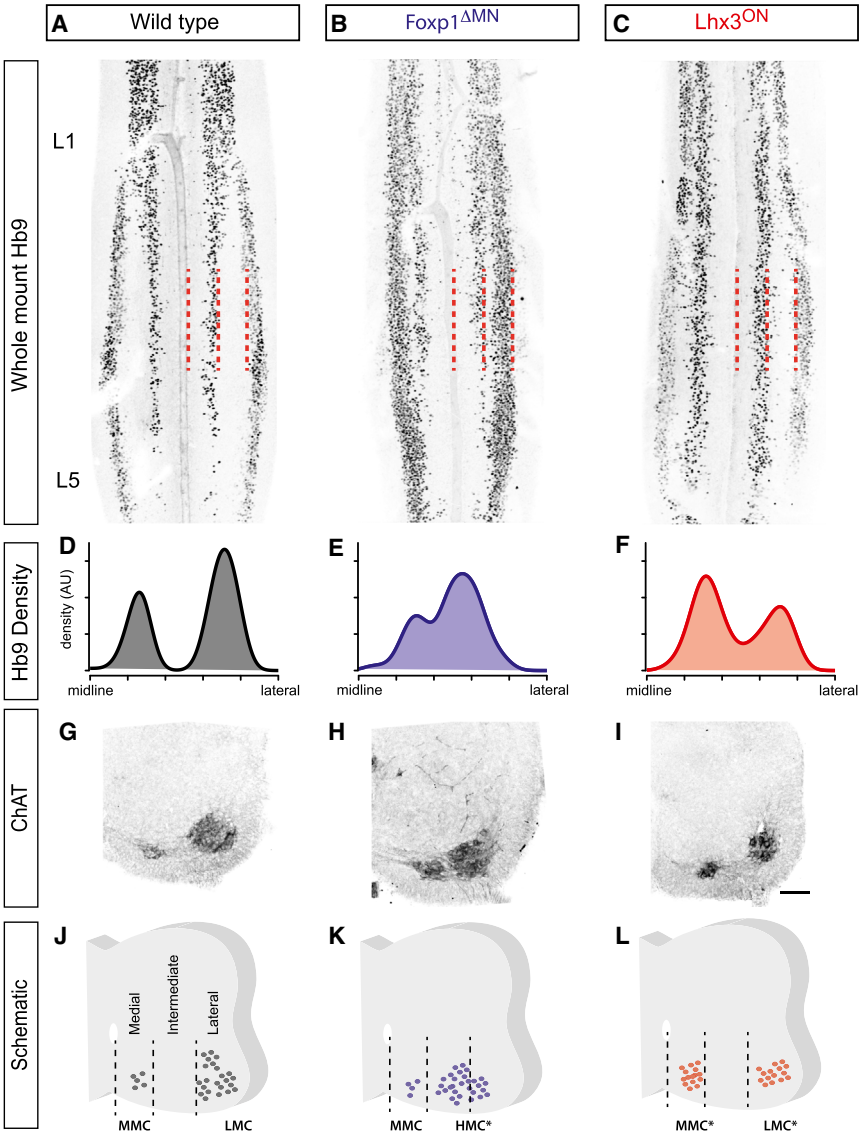

Figure 5. Lumbar Motor Column Structure

(A–C) Lumbar motor column structure revealed by whole mount Hb9 antibody staining in wild-type (A), Foxp1 $^{\Delta MN}$ (B), and Lhx3^{ON} (C) spinal cords.

(D–F) Plots of motorneuron density on the mediolateral axis in the mid lumbar spinal cord. Peaks in the density plots reflect the columnar organization of motorneuron somata detected by Hb9 immunostaining in wild type (D), Foxp1 $^{\Delta MN}$ (E), and Lhx3^{ON} (F) spinal cords.

(G–I) Lumbar motor column structure revealed by ChAT immunostaining of transverse sections in wild-type (G), Foxp1 $^{\Delta MN}$ (H), and Lhx3^{ON} (I) spinal cords. Scale bar, 100 μm.

(J–L) Wild-type spinal cords are characterized by two distinct motor columns spanning the lumbar enlargement, with a larger number of motorneurons in the LMC relative to the MMC (J). In the Foxp1$^{\Delta MN}$ spinal cord MMC cells are unaffected but LMC motorneurons settle more medially an in ectopic position (HMC*) and are absent from lateral positions (K). Motorneuron in Lhx3^{ON} spinal cords form distinct lateral (LMC*) and medial (MMC*) columns although their relative sizes are altered (L).

motorneurons in the positions occupied by the MMC and LMC, respectively. Interestingly, we found that despite their MMC-like genetic profile (Lhx3^{+}/Lhx4^{+}/Lhx1^{-}/Er81^{-}), laterally positioned Lhx3^{ON} motorneurons were Foxp1^{+}, while the enlarged medial column was Foxp1^{-} (Figure S4) (Sharma et al., 2000). Since the medial column in *Lhx3^{ON}* mice is comprised of both endogenous MMC motorneurons and respecified LMC cells, we have designated this the MMC*. Likewise, the lateral column in these mutant mice, which contains motorneurons with an abnormal columnar identity relative to their columnar position, has been labeled the LMC*.

We crossed the *Hb9::GCaMP6f* transgene into the *Lhx3^{ON}* background and imaged the spatial-temporal activity patterns of ~5,000 *Lhx3^{ON}* GCaMP6f -expressing motorneurons in E18.5 spinal cords (n = 8). Similar to wild-type littermates, rhythmic fluorescent oscillations were detected following neurochemical CPG activation, which were phase locked to electrically recorded contralateral ventral root bursts (Figures 7A and 7B). Similar to both wild-type and *Foxp1$^{\Delta MN}$* mutants, we found that most motorneurons were rhythmically active within the LMC* (94.6% ± 4.2%) and MMC* (91.8% ± 7%) in *Lhx3^{ON}* mice. Consistent with observations made with *Foxp1$^{\Delta MN}$* mutants, we found that rhythmic left-right coordinated motor activity is preserved in *Lhx3^{ON}* mice regardless of motorneuron subtype identity or position (Figure 7B).

Next, we examined whether the CPG inputs that coordinate flexor-extensor activity were dependent on an appropriate match between motorneuron subtype identity and position. We focused our analysis on the L3-L4 spinal levels because these segments contain significant numbers of the three columnar types responsible for lumbar locomotor activity (MMC, LMCl, and LMCm), facilitating the comparison of relative activity patterns across motorneuron subtypes. Nearly all *Lhx3^{ON}* MMC* motorneurons were flexor active, similar to the phasic pattern of wild-type MMC neurons (Figure 7C). When we determined the burst phase distributions of LMC* motorneurons in *Lhx3^{ON}* mice, we found a bimodal distribution with LMC* neurons active in the flexor and extensor phases of the locomotor cycle (Figure 7D). This distribution, however, was distinct from that observed for the wild-type LMC, reflecting an increased number of LMC* cells that were active in an intermediate phase between the main flexor and extensor phase peaks (Figure 7D, gray cells) and a reduction in the phase separation between the flexor and extensor phase peaks (Figure 7D, $p < 0.001$). These observations reveal an erosion of the distinct activity patterns that characterize flexor

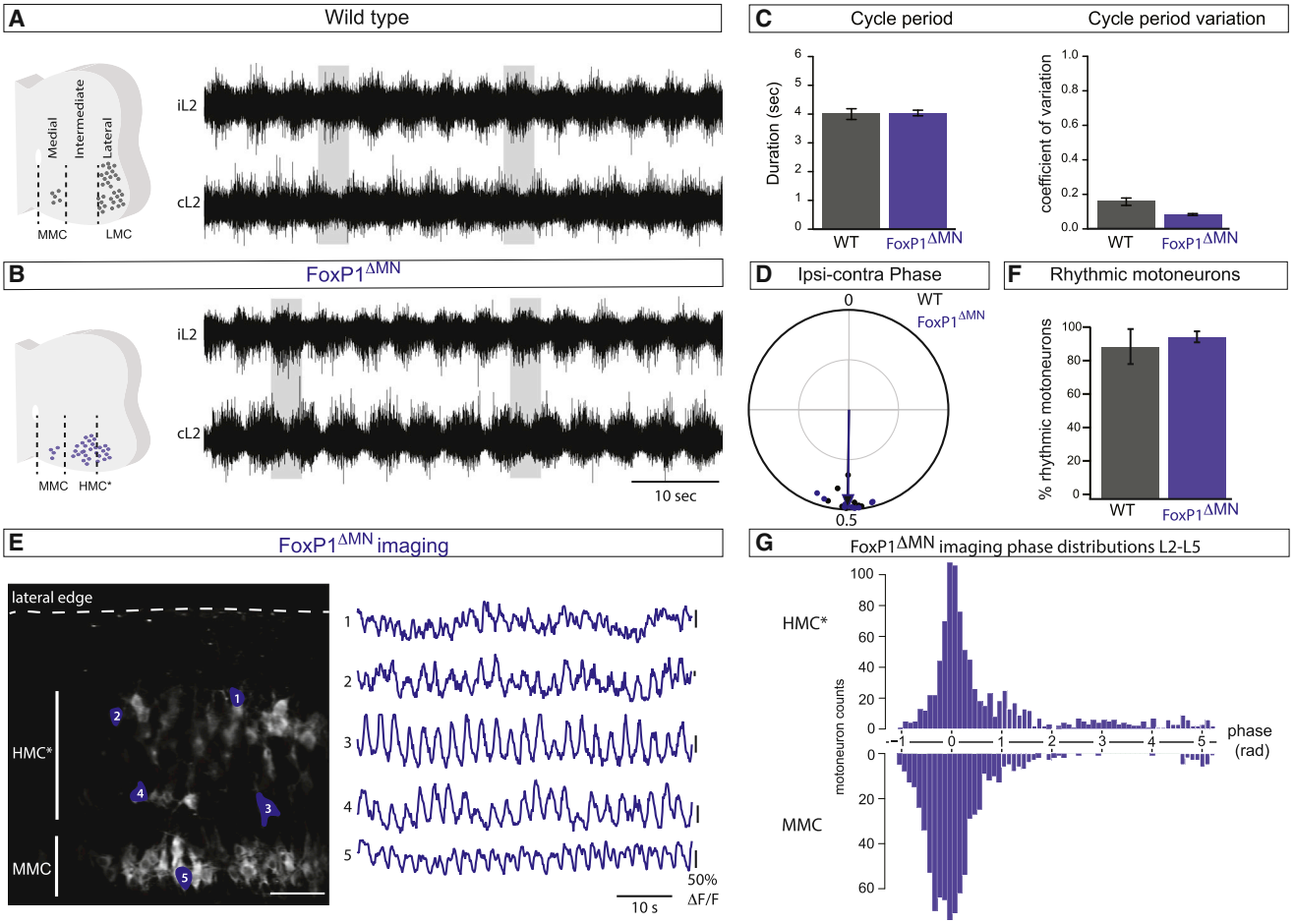

Figure 6. Locomotor Network Activity Is Preserved for Motorneurons in Ectopic Positions

(A) Neurochemically evoked fictive locomotor bursting recorded from the ventral roots in a wild-type E18.5 spinal cord. Rhythmic bursts of activity alternate between ipsi and contralateral ventral roots (iL2, cL2).

(B) Neurochemically evoked alternating, rhythmic bursting is retained in Foxp1$^{\Delta MN}$ spinal cords.

(C) Wild-type and Foxp1$^{\Delta MN}$ spinal cord fictive locomotor activity was not significantly different in cycle period (wild-type 4.04 ± 0.2 s; Foxp1$^{\Delta MN}$ 4.0 ± 0.1 s, p = 0.96) or in cycle variability (wild-type 0.12 ± 0.02: Foxp1$^{\Delta MN}$ 0.08 ± 0.007; p = 0.12; coefficient of variation). Means ± SEM.

(D) In Foxp1$^{\Delta MN}$ spinal cords ipsi and contralateral L2 bursting alternates (blue) with mean phases clustered around 0.5 cycles, similar to wild-type bursting (black). Points represent average values from ~20 cycles in single spinal cords.

(E) Image of GCaMP6f expressing Foxp1$^{\Delta MN}$ motorneurons in L4. GCaMP6f signals from the highlighted Foxp1$^{\Delta MN}$ motorneurons revealed coordinated, network driven oscillations in Foxp1$^{\Delta MN}$ motorneurons independent of their medial-lateral positions.

(F) Similar fractions of wild-type and Foxp1$^{\Delta MN}$ motorneurons are rhythmically active during neurochemically induced locomotor activity (88.4% ± 10.5% wild-type; 94.2% ± 3.3% Foxp1$^{\Delta MN}$; p = 0.09, mean ± SD).

(G) Phase distributions of L2-L5 HMC* and MMC in *Foxp1$^{\Delta MN}$* spinal cords. Similar proportions of HMC* and MMC are co active with L2 with phase values between 0 ± 1 radians. (p = 0.21).

and extensor alternation, following a loss of normal LMC identity. If motorneuron position is sufficient to specify the phasic bursting pattern, we expected to find a mediolateral distribution of cells within the LMC* that resembled the LMCl-flexor and LMCm-extensor arrangement in wild-type mice (Figure 4). We generated plots of motorneuron position and categorized each neuron by its activity phase. In the wild-type spinal cord, we observed a well-organized mediolateral segregation of LMC neurons, with flexor-phase motorneurons occupying the lateral most positions and extensor-phase cells in medial positions (Figures 7E and 7G, p = 0.0063; Movie S1). In contrast, analysis of *Lhx3^{ON}* mice revealed that flexor and extensor motorneurons were intermingled within the LMC* (Figure 7F; Movie S2). Comparison of the mediolateral distributions of *Lhx3^{ON}* motorneurons revealed no significant spatial separation between and flexor- and extensor-active cells (Figure 7H, p = 0.21). In addition, we found that intermediate phase neurons (i.e., rhythmic cells with neither flexor nor extensor bursts) were intermixed with flexor and extensor active LMC* neurons (Figure 7F, black cells), further obscuring the activity-position relationships observed in wild-type animals. Therefore, the discordance between cell identity and position not only causes a breakdown in the spatial organization of

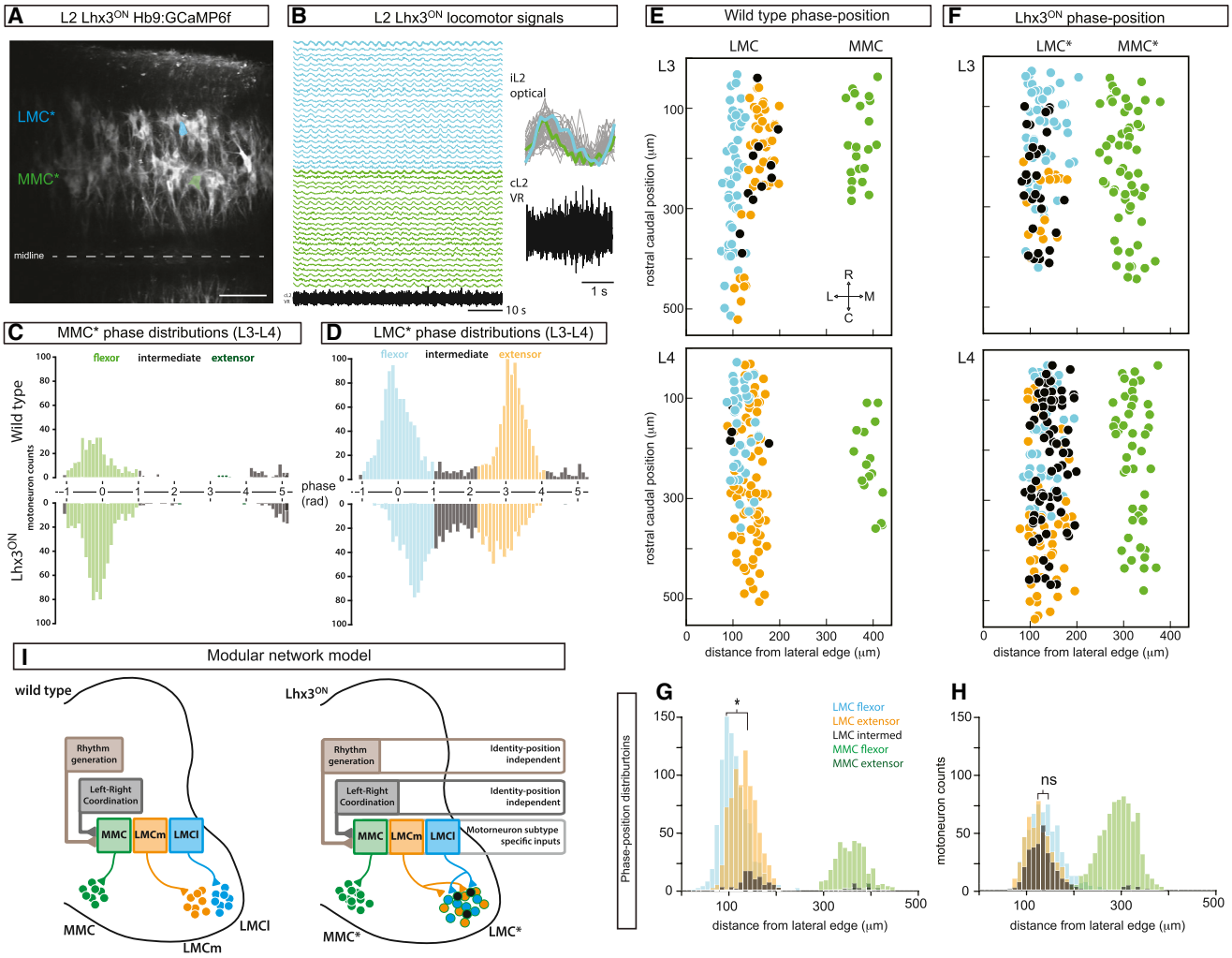

Figure 7. Imaging Lhx3^{ON} Locomotor Activity

(A) Single optical section of Hb9:GCaMP6f expressing Lhx3^{ON} L2 motorneurons. Example LMC* (cyan) and MMC* (green) neurons are highlighted. Scale bar 100 μm.

(B) Locomotor activity traces from the image in A. Fluorescence oscillations of LMC* (cyan) and MMC* (green) alternate with contralateral L2 ventral root activity (black). Cells highlighted in A are in bold. Inset, single locomotor cycle from imaging traces and contralateral L2 ventral root recording showing the stereotypical anti-phase relationship between ipsi and contralateral L2 activity patterns.

(C) Phase distributions of wild-type and Lhx3^{ON} L3-L4 MMC neurons. Similar to the wild-type MMC, a majority of Lhx3^{ON} MMC* motorneurons are flexor active (in phase with L2 imaging signals), with phase values clustered near zero.

(D) Comparison of wild-type and Lhx3^{ON} LMC phase distributions. The activity of L3-L4 LMC motorneurons in the wild-type spinal cord coalesces into flexor and extensor active populations. Flexor and extensor active LMC* are found in similar proportions to wild-type. In the Lhx3^{ON} spinal cord increased numbers of intermediate phase LMC* (neither flexor nor extensor) were observed relative to wild-type LMC (black bars). Wild-type, median 1.97%, range 0%–9.4% of LMC; Lhx3^{ON}, median 17.63%, range 1.7%–24.4%, p = 0.047.

(E and F) Reconstructions of motorneuron activity phase in L3 (top), and L4 (bottom). Points are individual motorneuron positions colored by activity phase. Reconstructions are aligned in the medial-lateral axis relative to the lateral edge of the spinal cord. Flexor phase: LMC, cyan; MMC, green; extensor phase: LMC, orange; intermediate phase, black. (E) In the wild-type cord, flexor active motorneurons (cyan) are generally lateral to extensor motorneurons (orange). (F) In the Lhx3^{ON} spinal cord, the mediolateral segregation of flexor and extensor neurons is lost. Intermediate phase neurons (black) are also intermingled with flexor (cyan) and extensor (orange) active LMC*.

(G and H) Summary histograms of L3-L4 motorneuron positions and activity classifications. In the wild-type spinal cord, the positions of flexor active LMCl (cyan) are shifted laterally relative to extensor active LMCm (orange, *p = 0.0063). In the Lhx3^{ON} spinal cord, flexor, extensor and intermediate active motorneurons are intermingled with similar positions on the medio-lateral axis (ns, p = 0.21).

(I) Specific modules of the locomotor CPG have distinct dependencies on motorneuron position and identity. Core features of the CPG network, rhythmic drive and left-right coordination, are wired independently of motorneuron identity and position; however, normal musculotopic motorneuron activity patterns are not preserved in the absence of proper LMC identity in Lhx3^{ON} mutants. Loss of lateral motorneuron identity generates new activity patterns (black) potentially from abnormal mixing of inputs onto motorneurons.

motorneurons with different burst phases, it also causes some cells to acquire novel patterns of activity. Although a loss of normal LMC identity does not preclude individual neurons from integrating into the CPG circuits that coordinate the burst phase among motorneurons, our analysis indicates that motorneuron position alone is not the sole determinant of phase.

DISCUSSION

Developmental studies have identified genetic programs that specify neuronal identity and regulate cell position, but these properties are intertwined, making it difficult to establish the precise cellular and molecular features that are used to build functional circuits. In this report, we have examined whether the orderly musculotopic arrangement of motorneurons is a primary determinant for establishing inputs from the CPG that drive coordinated muscle activation patterns for hind limb stepping. GCaMP6f imaging was used to monitor the activity of individual motorneurons within the medial and lateral motor columns. We found that the CPG drives specific patterns of motor bursts in which motorneuron columnar position is tightly correlated with burst phase. Using *Foxp1*$^{\Delta MN}$ and *Lhx3*^{ON} mice to genetically perturb motorneuron position and identity, we found that neither correct cell position nor proper subtype identity are necessary to establish rhythmic left/right-coordinated CPG-driven motor output. In contrast, the stereotypical relationship between cell position and burst phase across the mediolateral axis of the LMC is disrupted in *Lhx3*^{ON} mice. Thus, cell position and burst phase are not irrevocably linked, implying that motorneuron subtype identity is a recognition feature used for some, but not all, aspects of CPG wiring. Our results support growing evidence that the hind limb CPG can be subdivided into functional subcomponents for rhythm, left-right coordination, and flexor-extensor control based on the stringency of information extracted from motorneuron position and subtype identity used to guide the development of intra-spinal circuits for limb movement (Figure 7I) (McCrea and Rybak, 2008; Grillner and Jessell 2009; Kiehn, 2006; Garcia-Campmany et al., 2010).

The Spatiotemporal Structure of Spinal Motorneuron Activity

Here we report the first inter-columnar, large-scale cellular-resolution study of the mouse lumbar-spinal motorneuron network during fictive locomotion. Although the spatial organization of motorneurons and timing of motor pool activation have been indirectly calculated based on EMG recordings taken from muscles during locomotion (Yakovenko et al., 2002), these activation patterns reflect the integration of multiple premotor systems including descending, sensory, and local circuitries. We monitored the activity pattern of individual motorneurons in a preparation that isolates the activity of the lumbar CPG from other sources of motor control and used a reliable neurochemical method to activate the CPG circuitry that previous studies have found to engage similar interneuronal networks as those used during normal locomotion (Kullander et al., 2003; Gosgnach et al., 2006; Crone et al., 2009; Talpalar et al., 2013; Zhang et al., 2014). This approach has allowed us to disentangle specific layers of the CPG circuitry that contribute to patterned motor outputs (Figure 7I).

The known location of LMC motor pools and timing of limb muscle contractions predicts a rostral-flexor and caudal-extensor spatiotemporal pattern of motorneuron firing during walking (Yakovenko et al., 2002). The coordination between flexor and extensor classes of LMC motorneurons forms the basis for controlling the swing and stance portions of the step cycle. As expected, we found that activation of the CPG in an isolated spinal preparation produced a rostral-flexor and caudal-extensor distribution of motorneuron phases. Although the ventral root is comprised of motor axons from multiple columnar subtypes at each lumbar segment, the prevalence of LMCl motorneurons at L2 and LMCm at L5 generates a composite pattern of motor activity detected with ventral root recordings that is in good agreement with the burst relationships defined using GCaMP6f to monitor the activity of individual cells within the LMCl and LMCm. Motorneurons that innervate the axial musculature to support posture and maintain balance are located within the MMC. We found that MMC neurons are co-active during LMC flexor firing. However, unlike the LMC, the MMC does not display an obvious rostrocaudal phase transition from L2 to L5. Therefore, we have found that both inter and intra-columnar phase differences generate heterogeneous distributions of motorneuron activity in most lumbar segments, suggesting that the CPG circuitry uses more sophisticated means than simple rostrocaudal coordinates to pattern the motor output sequence within each segment.

By activating the CPG and examining the firing of individual motorneurons across the lumbar spinal cord, we found that a substantial majority of these neurons become activated during fictive locomotion. In particular, each columnar subtype displayed a similarly high proportion of bursting motorneurons regardless of spinal cord level. The CPG appears to be capable of serving as a major source of premotor input to all motorneurons regardless of subtype identity, columnar position, or rostrocaudal location. We found that the phase distribution of motor bursts mapped across the mediolateral axis of the LMC such that flexor-active motorneurons were situated laterally within the LMCl and extensor active neurons were present medially in the LMCm. Antagonistic pairs of muscles are innervated by motorneurons with different LMC subtype identities suggesting that a core feature in the generation of normal motor activity patterns is the differential recruitment of motorneurons based on their columnar identity. Our results reveal that the intrinsic spinal CPG circuit is sufficient to generate this basic template of motorneuron recruitment. We have performed extensive analyses using amplitude covariance methods, principle component analysis, and phase monitoring to unbiasedly extract imaging signal profiles associated with the individual motor pools within each motor column. Despite this effort, we failed to detect pool-specific activity patterns within motor columns following stimulation of the CPG. For example, under our experimental conditions, we failed to detect a consistent population of biphasically active LMC neurons, an activity profile that would facilitate the identification of specific motor pools within a motor column (data not shown). This failure may simply be a technical issue due, for example, to a lack of signal resolution with the GCaMP6f reporter. Nevertheless, it may also be the case that the isolated CPG driven by neurochemicals lacks the ability to consistently

regulate the fine level of coordination that occurs among motor pools during stepping. Additional inputs such as those from the premotor circuits in the dorsal spinal cord that relay sensory and descending motor commands might have a critical role in setting the timing of motor pool bursts within each motor column to generate complex motor behavior (Levine et al., 2014; Tripodi et al., 2011; Bourane et al., 2015; Betley et al., 2009; Akay et al., 2014; Hantman and Jessell, 2010; Zagoraiou et al., 2009).

Circuit Activity Independent of Motorneuron Identity and Position

Here, we leverage two independent genetic strategies to dissociate the relationship between motorneuron identity and position. Selective deletion of Foxp1 from motorneurons in *Foxp1*$^{\Delta MN}$ mice does not prevent motorneuron development, but it leads to a homeotic transformation in which an ectopic class of thoracic motorneurons, the HMC*, forms in the lumbar spinal cord at the expense of LMC cells (Dasen et al., 2008; Rousso et al., 2008). The majority of lumbar motorneurons in *Foxp1*$^{\Delta MN}$ mice are located in an abnormal medial position normally devoid of motorneurons and have a columnar subtype identity that is typically not found in the lower segments of the lumbar spinal cord. Despite the radical changes caused by *Foxp1* deletion, the ectopic misspecified motorneurons are efficiently driven to burst rhythmically with normal left-right alternation following CPG activation (Machado et al., 2015). Thus, these core features of the CPG circuitry appear to show little regard for motorneuron subtype identity or precise musculotopic positioning within the ventral horn. The cellular underpinnings of the CPG that mediate rhythmic alternating motor bursts have begun to be identified. Silencing the output of V3 interneurons disrupts rhythmic motor activity (Zhang et al., 2008). Conversely, ablation of V0 interneurons disrupts left-right coordination, while leaving the rhythm intact (Talpalar et al., 2013). Although the mechanisms that underlie V3 and V0 connectivity are not known, our studies indicate that these particular interneurons are relatively insensitive to motorneuron position and subtype identity. Rhythm generation and left-right coordination are fundamental features of the CPG circuit found in ancestral vertebrates lacking limbs and LMC motorneurons (Grillner and El Manira, 2015). Thus, these modules of the CPG may have evolved to drive motor activity regardless of their subtype identity.

The flexor-dominated phasing of HMC* motorneurons in *Foxp1*$^{\Delta MN}$ mice has led to the suggestion that the flexor components of the CPG circuitry are the primitive starting point for building flexor-extensor control in limbed vertebrates (Machado et al., 2015). By comparing the activity of the Foxp1-independent MMC and *Foxp1*$^{\Delta MN}$ HMC* motorneurons, our findings provide further perspective on the default regulation of burst phases. We found that the axial-controlling MMC and flexor-LMCl burst during the same phase; however, we noticed that the two motor columns displayed distinct patterns from one another based on their burst amplitude variations. Since recent synaptic-tracing studies have detected divergent inputs to motorneurons within the LMCl and MMC, it is likely that the interneuronal regulation of axial and flexor musculature is controlled differently (Goetz et al., 2015). Thus, an alternative possibility for the evolution of CPG circuitry is that the ancestral starting point was the interneuronal system that controls axial bending for swimming movements that is mediated by the MMC. These two scenarios of CPG evolution might be further informed using synaptic tracing in *Foxp1*$^{\Delta MN}$ mice to determine whether the inputs to the ectopic lumbar HMC* cells default to the flexor LMCl pattern or the axial MMC pattern.

Although flexor-extensor control of the hind limbs is absent in *Foxp1*$^{\Delta MN}$ mice, it is not clear whether this defect originates from abnormal sensory feedback, mislocalization of motorneurons, and/or misspecification of motorneuron identity (Sürmeli et al., 2011; Dasen et al., 2008; Rousso et al., 2008). We employed a complementary genetic strategy to examine whether the position of a motorneuron dictates the premotor input for flexor-extensor coordination among limb-innervating motorneurons in the LMC. We maintained the expression of Lhx3 in all lumbar motorneurons using *Lhx3*^{ON} mice, which creates a LIM transcription factor code for MMC identity (Tsuchida et al., 1994; Sharma et al., 1998, 2000). By preventing the downregulation of Lhx3, many LMC motorneurons relocate into the MMC, which we designate as the MMC* because it is enlarged approximately 2- to 3-fold and contains respecified LMC cells in addition to the normal MMC neurons. Nearly all of the cells in the MMC* were rhythmic, left-right coordinated, and displayed the same burst phase as normal MMC motorneurons. Thus, the premotor inputs that control MMC activity appear to have a degree of plasticity that makes them relatively insensitive to motorneuron number within this column.

Interestingly the conversion of LMC neurons to MMC cells is not completely penetrant in *Lhx3*^{ON} mice, resulting in cells with a partial MMC-gene profile (Lhx3^{+}/Lhx4^{+}/Lhx1^{-}/Foxp1^{+}) settling in an LMC position (Figure S4; Sharma et al., 2000). We term this motorneuron column the LMC*, as it contains cells in which "identity," as defined by several gene expression markers, has been dissociated from position. We found that the motorneurons within the LMC* of *Lhx3*^{ON} mice had lost the strict relationship between cell position and burst phase across the mediolateral axis of the LMC. Since V2b and V1 interneurons have been implicated in flexor-extensor control (Zhang et al., 2014), it is possible that their connectivity relies on an intact LMC identity. We did not find that the LMC* cells had all become phase locked with the MMC, suggesting that the incomplete reprogramming of MMC identity in *Lhx3*^{ON} mice interfered with a wholesale conversion to an MMC input pattern. Interestingly, in addition to flexor- and extensor-active motorneurons within the LMC*, we found a marked increase in the number of LMC* cells that were active during intermediate burst phases compared to controls. The abnormal burst phases displayed by these LMC* cells could be due to the conflict between cell position and cell identity and may possibly reflect the cumulative integration of LMCm, LMCl, and MMC inputs (Figure 7I).

Taken together, our findings demonstrate that motorneuron position is not sufficient to establish the fully patterned activity of the CPG. Consistent with previous studies indicating the CPG is modular with components for producing rhythm, coordinating left-right stepping, and mediating flexor-extensor control (Figure 7I), we found that the components for rhythm and

left-right control are relatively insensitive to motor neuron position and subtype identity. In contrast, the CPG components that mediate flexor-extensor control seem to require the proper matching of both motorneuron position and subtype identity. This modularity may extend to the relative weighting of the flexor and extensor drive produced by the CPG. We found that the isolated CPG is not limited to producing bursts during just flexion or extension; rather, many cells in the LMC* were rhythmically active during different phases. Although the CPG is often viewed as a rather rigid circuit that drives repetitive motor activity, the ability to combine different modules as needed may allow it to drive highly complex motor behaviors under the proper conditions.

EXPERIMENTAL PROCEDURES

All experiments were done in accordance with Institutional Animal Care and Use Committee animal protocols.

Spinal Cord Preparation

Spinal cords from E18.5–P2 mice were isolated in 4°C dissecting ACSF. Dissected spinal cords were transferred to room temperature oxygenated recording solution. Prior to calcium imaging experiments, the ventral roots were unilaterally removed from the lumbar spinal cord to facilitate optical access to the lateral motor column. Fictive locomotor activity was induced by bath application of 10–20 μM serotonin (5-HT) and 5-10 μM N-methyl-DL-aspartate (NMA) following a 20 min recovery period at room temperature.

Two-Photon Imaging and Electrophysiology

Motorneuron activity was recorded from the ventral roots with suction electrodes and filtered from 100 Hz–3 kHz. Calcium imaging of motorneuron activity was conducted in GCaMP6f-expressing spinal cords using an upright two-photon microscope (Prairie Technologies) with a 20× 1.0 NA water-immersion objective (Olympus). GCaMP6f was excited at 920 nm through the ventral surface of the spinal cord. Calcium imaging was conducted at 8.3 frames/second with a field of view of ~550 × 550 μm unless otherwise noted. During imaging experiments, electrical activity was monitored by L2 and L5 ventral root recordings contralateral to the imaged motorneurons.

Immunohistochemistry

Isolated spinal cords were fixed in 4% PFA for 2–4 hr, washed in PBS, and prepared for cryosectioning or whole-mount staining. Whole spinal cords were incubated with primary and secondary antibodies for >3 days and then optically cleared (Hama et al., 2011). Fixed samples were imaged on an Olympus confocal microscope.

Data Analysis

All analysis was conducted with custom written pipelines in R using the igraph, signal, circular, and fpc function packages. The nonparametric Kolmogorov-Smirnov and Kruskal-Wallis Rank Sum tests were used to assess statistical differences. The Rayleigh test for circular uniformity and Watson's two-sample test for homogeneity were used for circular data. Motorneuron regions of interest were manually drawn in ImageJ and 60–100 s time series traces of imaging data were exported for further analysis.

Phase Categorization

The phase of imaging signals is plotted relative to the phase of L2 imaging signals in each experiment. We categorized imaging signals with a phase 0 ± 1 radians relative to L2 imaging to be flexor active, conversely imaging signals with a phase π +/1 radians relative to L2 imaging signals to be extensor active. Motorneurons with phase values outside these defined flexor and extensor ranges were categorized as intermediate and depicted with black bars/symbols in all figures.

SUPPLEMENTAL INFORMATION

Supplemental Information includes Supplemental Experimental Procedures, four figures, and two movies and can be found with this article online at http://dx.doi.org/10.1016/j.neuron.2015.08.005.

AUTHOR CONTRIBUTIONS

C.A.H. and S.L.P. designed the study. S.L.P., W.A.A., and B.W.G. designed a preliminary study of *Lhx3*^{ON} animals. C.A.H. conducted calcium-imaging experiments and electrophysiological recordings. W.A.A. and B.W.G. performed preliminary ventral root recordings. M.H. generated the *Hb9::GCaMP6f* mouse line and K.L.H. generated transgenic animals used in a preliminary version of this study. T.O.S. assisted with data analysis. S.P.D. designed and wrote analysis algorithms. J.D.D. and H.O.T. generated *Foxp1*$^{fl/fl}$ animals. C.A.H. and S.L.P. wrote the paper.

ACKNOWLEDGMENTS

C.A.H. was supported by an NRSA fellowship from NINDS (F32 NS070498). K.L.H. is a National Science Foundation Graduate Research Fellow. M.H. was supported by the Timken–Sturgis Foundation and the Japanese Ministry of Education, Culture, Sports, Science, and Technology Long-Term Student Support Program. S.L.P. is an HHMI investigator and Benjamin H. Lewis chair in neuroscience. This research was supported by the National Institute of Neurological Disorders and Stroke (grant R37NS037116), the Howard Hughes Medical Institute, the Christopher and Dana Reeve Foundation, the Marshall Foundation, and the Sol Goldman Charitable Trust.

Received: June 9, 2015
Revised: July 29, 2015
Accepted: August 3, 2015
Published: September 2, 2015

REFERENCES

Akay, T., Tourtellotte, W.G., Arber, S., and Jessell, T.M. (2014). Degradation of mouse locomotor pattern in the absence of proprioceptive sensory feedback. Proc. Natl. Acad. Sci. USA *111*, 16877–16882.

Betley, J.N., Wright, C.V.E., Kawaguchi, Y., Erdélyi, F., Szabó, G., Jessell, T.M., and Kaltschmidt, J.A. (2009). Stringent specificity in the construction of a GABAergic presynaptic inhibitory circuit. Cell *139*, 161–174.

Bonanomi, D., and Pfaff, S.L. (2010). Motor axon pathfinding. Cold Spring Harb. Perspect. Biol. *2*, a001735.

Bourane, S., Grossmann, K.S., Britz, O., Dalet, A., Del Barrio, M.G., Stam, F.J., Garcia-Campmany, L., Koch, S., and Goulding, M. (2015). Identification of a spinal circuit for light touch and fine motor control. Cell *160*, 503–515.

Chen, T.-W., Wardill, T.J., Sun, Y., Pulver, S.R., Renninger, S.L., Baohan, A., Schreiter, E.R., Kerr, R.A., Orger, M.B., Jayaraman, V., et al. (2013). Ultrasensitive fluorescent proteins for imaging neuronal activity. Nature *499*, 295–300.

Crone, S.A., Zhong, G., Harris-Warrick, R., and Sharma, K. (2009). In mice lacking V2a interneurons, gait depends on speed of locomotion. J. Neurosci. *29*, 7098–7109.

Dasen, J.S., and Jessell, T.M. (2009). Hox networks and the origins of motor neuron diversity. Curr. Top. Dev. Biol. *88*, 169–200.

Dasen, J.S., De Camilli, A., Wang, B., Tucker, P.W., and Jessell, T.M. (2008). Hox repertoires for motor neuron diversity and connectivity gated by a single accessory factor, FoxP1. Cell *134*, 304–316.

Fukuhara, K., Imai, F., Ladle, D.R., Katayama, K., Leslie, J.R., Arber, S., Jessell, T.M., and Yoshida, Y. (2013). Specificity of monosynaptic sensory-motor connections imposed by repellent Sema3E-PlexinD1 signaling. Cell Rep. *5*, 748–758.

Garcia-Campmany, L., Stam, F.J., and Goulding, M. (2010). From circuits to behaviour: motor networks in vertebrates. Curr. Opin. Neurobiol. *20*, 116–125.

Goetz, C., Pivetta, C., and Arber, S. (2015). Distinct limb and trunk premotor circuits establish laterality in the spinal cord. Neuron *85*, 131–144.

Gosgnach, S., Lanuza, G.M., Butt, S.J.B., Saueressig, H., Zhang, Y., Velasquez, T., Riethmacher, D., Callaway, E.M., Kiehn, O., and Goulding, M. (2006). V1 spinal neurons regulate the speed of vertebrate locomotor outputs. Nature *440*, 215–219.

Goulding, M. (2009). Circuits controlling vertebrate locomotion: moving in a new direction. Nat. Rev. Neurosci. *10*, 507–518.

Grillner, S., and El Manira, A. (2015). The intrinsic operation of the networks that make us locomote. Curr. Opin. Neurobiol. *31*, 244–249.

Grillner, S., and Jessell, T.M. (2009). Measured motion: searching for simplicity in spinal locomotor networks. Curr. Opin. Neurobiol. *19*, 572–586.

Hama, H., Kurokawa, H., Kawano, H., Ando, R., Shimogori, T., Noda, H., Fukami, K., Sakaue-Sawano, A., and Miyawaki, A. (2011). Scale: a chemical approach for fluorescence imaging and reconstruction of transparent mouse brain. Nat. Neurosci. *14*, 1481–1488.

Hantman, A.W., and Jessell, T.M. (2010). Clarke's column neurons as the focus of a corticospinal corollary circuit. Nat. Neurosci. *13*, 1233–1239.

Hayes, H.B., Chang, Y.-H., and Hochman, S. (2009). An in vitro spinal cord-hindlimb preparation for studying behaviorally relevant rat locomotor function. J. Neurophysiol. *101*, 1114–1122.

Hollyday, M. (1980). Organization of motor pools in the chick lumbar lateral motor column. J. Comp. Neurol. *194*, 143–170.

Jessell, T.M., Sürmeli, G., and Kelly, J.S. (2011). Motor neurons and the sense of place. Neuron *72*, 419–424.

Kiehn, O. (2006). Locomotor circuits in the mammalian spinal cord. Annu. Rev. Neurosci. *29*, 279–306.

Kiehn, O., and Kjaerulff, O. (1996). Spatiotemporal characteristics of 5-HT and dopamine-induced rhythmic hindlimb activity in the in vitro neonatal rat. J. Neurophysiol. *75*, 1472–1482.

Kjaerulff, O., and Kiehn, O. (1996). Distribution of networks generating and coordinating locomotor activity in the neonatal rat spinal cord in vitro: a lesion study. J. Neurosci. *16*, 5777–5794.

Klein, D.A., Patino, A., and Tresch, M.C. (2010). Flexibility of motor pattern generation across stimulation conditions by the neonatal rat spinal cord. J. Neurophysiol. *103*, 1580–1590.

Kullander, K., Butt, S.J.B., Lebret, J.M., Lundfald, L., Restrepo, C.E., Rydström, A., Klein, R., and Kiehn, O. (2003). Role of EphA4 and EphrinB3 in local neuronal circuits that control walking. Science *299*, 1889–1892.

Ladle, D.R., Pecho-Vrieseling, E., and Arber, S. (2007). Assembly of motor circuits in the spinal cord: driven to function by genetic and experience-dependent mechanisms. Neuron *56*, 270–283.

Landmesser, L., and Morris, D.G. (1975). The development of functional innervation in the hind limb of the chick embryo. J. Physiol. *249*, 301–326.

Lanuza, G.M., Gosgnach, S., Pierani, A., Jessell, T.M., and Goulding, M. (2004). Genetic identification of spinal interneurons that coordinate left-right locomotor activity necessary for walking movements. Neuron *42*, 375–386.

Lee, S.-K., Jurata, L.W., Funahashi, J., Ruiz, E.C., and Pfaff, S.L. (2004). Analysis of embryonic motoneuron gene regulation: derepression of general activators function in concert with enhancer factors. Development *131*, 3295–3306.

Levine, A.J., Hinckley, C.A., Hilde, K.L., Driscoll, S.P., Poon, T.H., Montgomery, J.M., and Pfaff, S.L. (2014). Identification of a cellular node for motor control pathways. Nat. Neurosci. *17*, 586–593.

Machado, T.A., Pnevmatikakis, E., Paninski, L., Jessell, T.M., and Miri, A. (2015). Primacy of flexor locomotor pattern revealed by ancestral reversion of motor neuron identity. Cell *162*, 338–350.

McCrea, D.A., and Rybak, I.A. (2008). Organization of mammalian locomotor rhythm and pattern generation. Brain Res. Brain Res. Rev. *57*, 134–146.

McHanwell, S., and Biscoe, T.J. (1981). The localization of motoneurons supplying the hindlimb muscles of the mouse. Philos. Trans. R. Soc. Lond. B Biol. Sci. *293*, 477–508.

Pecho-Vrieseling, E., Sigrist, M., Yoshida, Y., Jessell, T.M., and Arber, S. (2009). Specificity of sensory-motor connections encoded by Sema3e-Plxnd1 recognition. Nature *459*, 842–846.

Romanes, G.J. (1941). Cell columns in the spinal cord of a human foetus of fourteen weeks. J. Anat. *75*, 145–152.1, 1.

Romanes, G.J. (1951). The motor cell columns of the lumbo-sacral spinal cord of the cat. J. Comp. Neurol. *94*, 313–363.

Rousso, D.L., Gaber, Z.B., Wellik, D., Morrisey, E.E., and Novitch, B.G. (2008). Coordinated actions of the forkhead protein Foxp1 and Hox proteins in the columnar organization of spinal motor neurons. Neuron *59*, 226–240.

Schilling, N., and Carrier, D.R. (2010). Function of the epaxial muscles in walking, trotting and galloping dogs: implications for the evolution of epaxial muscle function in tetrapods. J. Exp. Biol. *213*, 1490–1502.

Sharma, K., Sheng, H.Z., Lettieri, K., Li, H., Karavanov, A., Potter, S., Westphal, H., and Pfaff, S.L. (1998). LIM homeodomain factors Lhx3 and Lhx4 assign subtype identities for motor neurons. Cell *95*, 817–828.

Sharma, K., Leonard, A.E., Lettieri, K., and Pfaff, S.L. (2000). Genetic and epigenetic mechanisms contribute to motor neuron pathfinding. Nature *406*, 515–519.

Smith, J.C., and Feldman, J.L. (1987). In vitro brainstem-spinal cord preparations for study of motor systems for mammalian respiration and locomotion. J. Neurosci. Methods *21*, 321–333.

Stepien, A.E., and Arber, S. (2008). Probing the locomotor conundrum: descending the 'V' interneuron ladder. Neuron *60*, 1–4.

Sürmeli, G., Akay, T., Ippolito, G.C., Tucker, P.W., and Jessell, T.M. (2011). Patterns of spinal sensory-motor connectivity prescribed by a dorsoventral positional template. Cell *147*, 653–665.

Talpalar, A.E., Bouvier, J., Borgius, L., Fortin, G., Pierani, A., and Kiehn, O. (2013). Dual-mode operation of neuronal networks involved in left-right alternation. Nature *500*, 85–88.

Thaler, J., Harrison, K., Sharma, K., Lettieri, K., Kehrl, J., and Pfaff, S.L. (1999). Active suppression of interneuron programs within developing motor neurons revealed by analysis of homeodomain factor HB9. Neuron *23*, 675–687.

Tripodi, M., Stepien, A.E., and Arber, S. (2011). Motor antagonism exposed by spatial segregation and timing of neurogenesis. Nature *479*, 61–66.

Tsuchida, T., Ensini, M., Morton, S.B., Baldassare, M., Edlund, T., Jessell, T.M., and Pfaff, S.L. (1994). Topographic organization of embryonic motor neurons defined by expression of LIM homeobox genes. Cell *79*, 957–970.

William, C.M., Tanabe, Y., and Jessell, T.M. (2003). Regulation of motor neuron subtype identity by repressor activity of Mnx class homeodomain proteins. Development *130*, 1523–1536.

Yakovenko, S., Mushahwar, V., VanderHorst, V., Holstege, G., and Prochazka, A. (2002). Spatiotemporal activation of lumbosacral motoneurons in the locomotor step cycle. J. Neurophysiol. *87*, 1542–1553.

Zagoraiou, L., Akay, T., Martin, J.F., Brownstone, R.M., Jessell, T.M., and Miles, G.B. (2009). A cluster of cholinergic premotor interneurons modulates mouse locomotor activity. Neuron *64*, 645–662.

Zhang, Y., Narayan, S., Geiman, E., Lanuza, G.M., Velasquez, T., Shanks, B., Akay, T., Dyck, J., Pearson, K., Gosgnach, S., et al. (2008). V3 spinal neurons establish a robust and balanced locomotor rhythm during walking. Neuron *60*, 84–96.

Zhang, J., Lanuza, G.M., Britz, O., Wang, Z., Siembab, V.C., Zhang, Y., Velasquez, T., Alvarez, F.J., Frank, E., and Goulding, M. (2014). V1 and v2b interneurons secure the alternating flexor-extensor motor activity mice require for limbed locomotion. Neuron *82*, 138–150.